

# Design and Finite Element Analysis of Mixed Aerofoil Wind Turbine Blades

Xinzi Tang, Ruitao Peng, Xiongwei Liu, Anthony Ian Broad

School of Computing, Engineering and Physical Sciences, University of Central Lancashire  
Fylde Road, Preston, UK

E-mail: {xtang4, rtpeng, xliu9}@uclan.ac.uk

**Keywords:** wind turbine blade design, finite element analysis.

## 1 INTRODUCTION

Wind turbine technology is one of the rapid growth sectors of renewable energy all over the world. As a core component of a wind turbine, it is a common view that the design and manufacturing of rotor blades represent about 20% of the total investment of the wind turbine [1]. Moreover, the performance of a wind turbine is highly dependent on the design of the rotor [2]. As well as rotor aerodynamic performance, the structure strength, stiffness and fatigue of the blade are also critical to the wind turbine system service life.

This paper presents the design and Finite Element Analysis (FEA) of a 10KW fixed-pitch variable-speed wind turbine blade with five different thickness of aerofoil shape along the span of the blade. The main parameters of the wind turbine rotor and the blade aerodynamic geometry shape are determined based on the principles of the blade element momentum (BEM) theory. Based on the FE method, deflections and strain distributions of the blade under extreme wind conditions are numerically predicted. The results indicate that the tip clearance is sufficient to prevent collision with the tower, and the blade material is linear and safe.

## 2 BLADE DESIGN

The wind turbine is a 10KW horizontal axis fixed-pitch variable-speed wind turbine. The design process of the three-bladed rotor initially comes with the determination of the rotor diameter and material.

### 2.1 Rotor Diameter and Material

The power extracted from the wind is proportional to the cube of wind speed as well as the area of the rotor. It is often preferable to have an effective rotor but not a too big one as the cost increases with the rotor size. In order to have an initialization of the efficiency of small wind turbines before any specific designs are conducted, it was suggested that the efficiency of modern wind turbine rotors

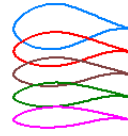
is generally about 30%-40% [3]. Assuming a rotor efficiency of 40% and a total efficiency of 33.8%, a diameter of 5m is selected for the 10KW wind turbine. And the material of the blade is resin-reinforced fiber glass due to easy local availability.

### 2.2 Blade Aerofoil Shape

For horizontal axis wind turbines, it is recommended to have a higher lift but lower drag aerofoil. There are many kinds of aerofoil including the general aviation aerofoil, such as NACA series, which are still used in some wind turbines. However, with the development of wind turbines, the dedicated aerofoil came about. The S series designed by NREL in USA, is mostly used in stall-regulated wind turbines for its gentle behavior in stall conditions; the FFA W series designed in Sweden and RIS series designed in Denmark, are preferable for lower Reynolds applications, and the DU series designed in Netherland, is popular in High Reynolds for large wind turbines. Each of these series has its own aerofoil shape with different thickness-to-chord ratio of 18%-40%. The thicker aerofoil shapes are often located at the inner part (close to rotor centre) of the blade while the thinner ones are set in the outer part of the blade due to ease of manufacturing and better strength and stiffness. The basic aerofoil (from 30% to 90% radius sections) selected in this wind turbine blade is DU93-W-210 which has a high lift-to-drag coefficient [4]. For similarity reason, the aerofoil shapes at other stations are also derived from the DU series by changing the thickness. The transition between sections is obtained by linear interpolation. The properties and distribution of these aerofoil shapes (named respectively DU93-W-210-40%, DU93-W-210-30%, DU93-W-210-25%, DU93-W-210, and DU93-W-210-18%) are listed in Table I. The aerodynamic coefficients derived from Xfoil are shown in Figure 1. The rest coefficients at high attack angles are extended by the Viterna-Corrigan method [5].

**Table 1:** Blade configuration

<i>Aerofoil Shapes</i>	<i>Thickness ratio</i>	<i>Aerofoil Shapes</i>	<i>Stations</i>
DU93-W-210-40%	40%		0.05R

Aerofoil Shapes	Thickness ratio	Aerofoil Shapes	Stations
DU93-W-210-30%	30%		0.1R
DU93-W-210_25%	25%		0.15R-0.3R
DU93-W-210	21%		0.35R-0.9R
DU93-W-210-18%	18%		0.95R-1R

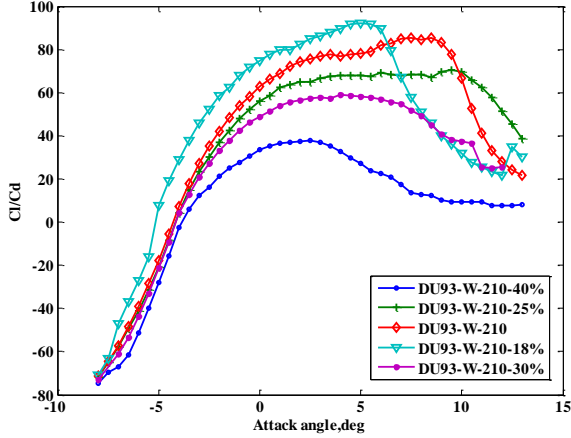


**Figure 1:** Aerodynamic coefficients  $C_l/C_d$  versus attack angles

### 2.3 Blade Chord and Twist

Given the rotor design parameters (e.g. rotor diameter, tip speed, aerofoil, rated wind speed and etc.), the main task of blade design is to determine the chord and twist distributions along the span of the blade. The optimal chords and twists are often calculated based on blade element momentum (BEM) theory. In this theory, complex flows are simplified into steady uniform conditions; and the total efficiency is integrated from several blade element sections which experience different flow velocity and different attack angle for the same hub wind speed. The integration equation is shown below [3]:

$$C_p = (8/\lambda^2) \int_{\lambda_h}^{\lambda} F_r \sin^2 \phi_r (\cos \phi_r - \lambda_r \sin \phi_r) (\sin \phi_r + \lambda_r \cos \phi_r) \lambda_r^2 [1 - (C_d/C_l) \cot \phi] d\lambda_r \quad (1)$$

Ignoring the drag and setting the partial derivative of the main part to zero, the optimum design equation for any kind of aerofoil can be obtained:

$$\phi_r = \left( \frac{2}{3} \right) \tan^{-1} \left( \frac{1}{\lambda_r} \right) \quad (2)$$

$$C_r = \frac{8\pi r}{N C_l} (1 - \cos \phi_r) \quad (3)$$

Where the  $C_p$  is the power coefficient,  $C_l$  is the lift coefficient,  $C_d$  is the drag coefficient,  $\lambda$  is the tip speed ratio,  $\phi$  is the angle of relative wind,  $N$  is the blade number and  $F$  is the tip loss factor. Subscript  $r$  represents position  $r/R$ ,  $h$  is hub position and  $t$  is tip position.

The design tip speed of wind turbine is considered to be theoretically as high as possible since an aerofoil produces

high lift at high Reynolds numbers; meanwhile, a lower tip speed is preferred to keep within noise limits. The design tip speed of this 10KW wind turbine is set to 68m/s. Aiming at an optimal power performance for an annual mean wind speed of 6m/s, the rated wind speed is set to 8.5m/s and the design tip speed ratio is 8. According to equation (2) and (3), as five different aerofoil shapes are employed, the initial chord and twist distribution showed non-continuous variations along the blade span and irregular chord length and twist angle appeared in the transition area between sections. This may cause bad effects both in aerodynamic and structure aspects: the aerodynamic flow over these blade sections is not two dimensional and may yield secondary loads and stress concentration. Furthermore, it looks rather poor when manufactured. Thus, the chords and twists of the main sections (0.35R-0.9R) are maintained, and the rest of the sections are obtained according to the basic aerofoil characteristics. Figure 2 shows the chord and twist distributions of the blade. Some small alternations have been made to the tip region which do not affect the power coefficients so much but would reduce thrusts at high winds. The twist angles of the tip region are set to be positive to have less thrust at high winds and better starting behaviours while the power coefficient is kept quite close to the theoretically optimum one.

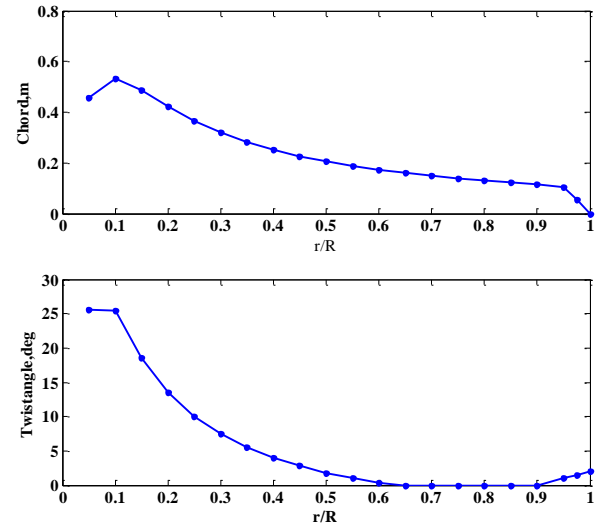


**Figure 2:** Blade chord and twist distributions

### 2.4 Power, torque and thrust coefficients

Following an optimal blade geometry design at an specific tip speed ratio, the power, torque, and thrust coefficients for the whole range of tip speed ratios are determined (as shown in Figure 3) from equation 4,5 and 6 [3]:

$$C_{Thrust} = \frac{8}{\lambda^2} \int_{\lambda_h}^{\lambda} F \lambda_r^3 a' (1-a) [1 - (C_d/C_l) \cot \phi_r] d\lambda_r \quad (4)$$

$$C_{Thrust} = \frac{\int_0^R \frac{1}{2} N \rho U_{rel}^2 (C_l \cos \phi_r + C_d \sin \phi_r) c dr}{0.5 \rho U_{rel}^2 \pi R^2} \quad (5)$$

$$C_{torque} = \frac{\int_0^R \frac{1}{2} N \rho U_{rel}^2 (C_l \sin \phi_r - C_d \cos \phi_r) c dr}{0.5 \rho U_{rel}^2 \pi R^2} \quad (6)$$

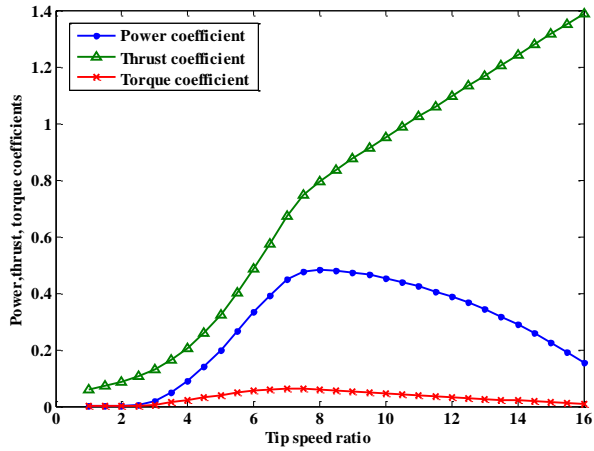


Figure 3: Power torque and thrust coefficients

#### 4 FINITE ELEMENT MODELING

The ultimate strength of the blade was analyzed via finite element modelling techniques as follows.

##### 4.1 Blade shell model

The blade geometry was modelled in CATIA, and the finite element model (FEM) was developed in ABAQUS, the structure of the blade was modelled with shell elements (S4R, capable of representing layer characteristics throughout the shell thickness).

The section view of components in layup schedule and the layup schedule were presented in Figure 4 and Table 2 respectively. According to section force characteristics, in order to improve the overall stiffness of the blade and increase the carrying capacity and prevent local buckling, spar cap and shear web structure were introduced. In the layup schedule, 0 degree plies were mainly used to withstand axial force, 45 degree plies mainly to withstand torque and shear forces.

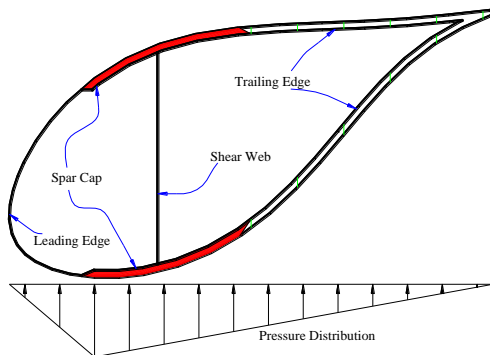


Figure 4: Display of components and pressure distribution

The material parameters were listed in Table 3[6], The A130, DB120 lamina were used for the 0 degree layups and  $\pm 45$  degree layups respectively, balsa wood was introduced as a filler in sandwich-type layups to minimize the weight. The failure criteria applied for designing the blade were based on failure strains parameters [6, 7].

Table 2: Layup schedule for the blade

Component	Radius (%)	Z location (mm)	Layup schedule	Thick ness
Root	2.8 to 5	140 to 250	$[\pm 45/0_6/\pm 45/0_6/+45]_s$	9.35
Spar cap	5 to 20	250 to 1000	$[\pm 45/0_6/\pm 45/0_6/+45]_s$	9.35
	20 to 40	1000 to	$[\pm 45/0_5/\pm 45/0_5/+45]_s$	7.5
	40 to 60	2000 to	$[\pm 45/0_4/\pm 45/0_4/+45]_s$	5.2
	60 to 80	3000 to	$[\pm 45/0_3/\pm 45/0_3/+45]_s$	3.85
	80 to	4000 to	$[\pm 45/0_2/\pm 45/0_2/+45]_s$	2.7
Leading edge	5 to 20	250 to 1000	$[\pm 45/0_2/\pm 45]_s$	3
	20 to	1000 to	$[\pm 45/0/\pm 45]_s$	1.85
Trailing edge	5 to 80	250 to 4000	$[\pm 45/0/\text{balsa}0/\pm 45]_s$	7
	80 to	4000 to	$[\pm 45/0]_s$	1.3
Shear web	5 to 100	250 to 5000	$[\pm 45/0_2/\pm 45]_s$	3

Table 3: Material parameters in the layups [5]

	$E_{11}/$ GPa	$E_{22}/$ GPa	$E_{33}/$ GPa	$\nu_{12}$	$\nu_{13}$	$\nu_{23}$	$G_{12}/$ GPa	$G_{13}/$ GPa	$G_{23}/$ GPa
A130	31.7	7.58	7.58	0.32	0.32	0.32	3.45	3.10	3.10
DB120	26.2	6.55	6.55	0.39	0.32	0.35	4.14	3.72	3.72
Balsa	0.187	0.06	4.07	0.67	0.02	0.01	0.02	0.22	0.15

##### 4.2 Loads prediction and definition

The loadings affecting a wind turbine blade are important in two primary areas including ultimate strength and fatigue. Limit loads in gusts are used to design the ultimate strength of blade; correspondingly normal running loads are utilized to design the fatigue strength. The blade was designed to survive an extreme wind speed of 60 m/s [8] with the wind turbine was not in operation. To model the blade load for a stationary wind turbine in such an extreme wind condition, the dynamic pressure on the high pressure side of the blade was introduced for the FE model, which defined as [6]:

$$P = 0.5 \times \rho \times v^2 \quad (7)$$

Where  $\rho$  is the air density (1.225 kg /m<sup>3</sup>),  $V$  is the wind velocity. A pressure distribution was applied to the blade model as shown in Figure 4.

In this study, for the layup schedule the static strength design of first layer was mainly taken into account. At the root end of the blade, all six degrees of freedom for the nodes in the root plane of the blade were fixed, and no other displacement constraints were imposed on the blade model.

##### 4.3 Results and discussion

Simulations were performed in the solver of Abaqus/Standard, Figure 5 and Figure 6 present the contour plot and distribution of displacement under the wind speed of 60 m/s, it shows that the displacement of blade sections increase from the root to the tip, the maximum displacement in flap-wise direction is 454 mm, meanwhile the minimum displacement position locates at the blade root, which meets the characteristics of the cantilever, and indicates that the tip clearance is sufficient to avoid collision with the tower.

When looking at the maximum in-plane principal strains of the blade, as shown in Figure 7, it is apparent that the maximum strain occurs at the blade root section as the

root experiences a larger load with a smaller area, however the strain is still much less than the ultimate strains of the material in layups. For weight consideration, thickness of layups rapidly declined in the direction from root to tip, which results in local strain discontinuous areas.

Figure 8 shows a linear relationship between load and tip displacement, the deformation of the blade linearly increases with rise in load, which again indicate the blade material is still linear and safe.

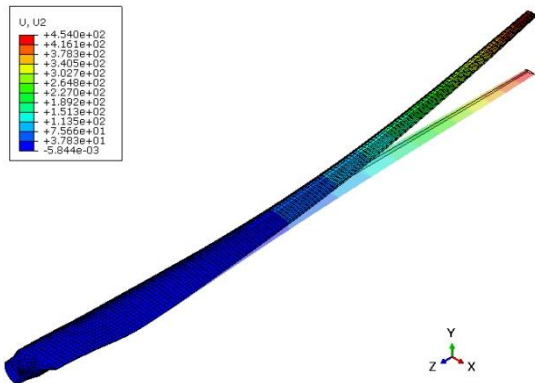


Figure 5: Distribution of displacement in flap-wise direction

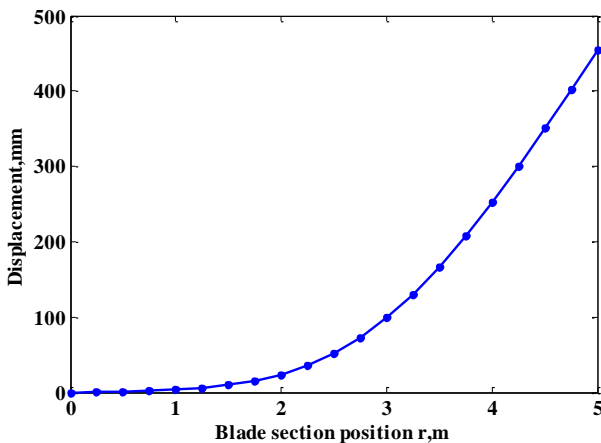


Figure 6: Displacements of sections

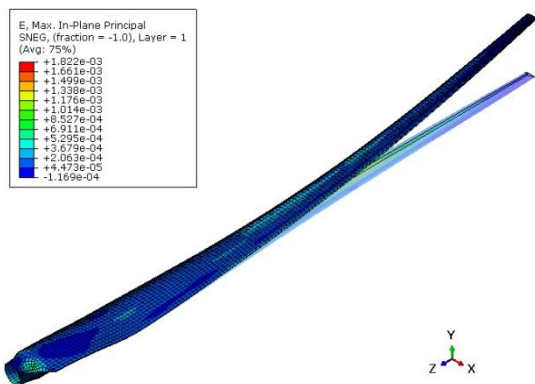


Figure 7: Distribution of maximum in-plane principal strain

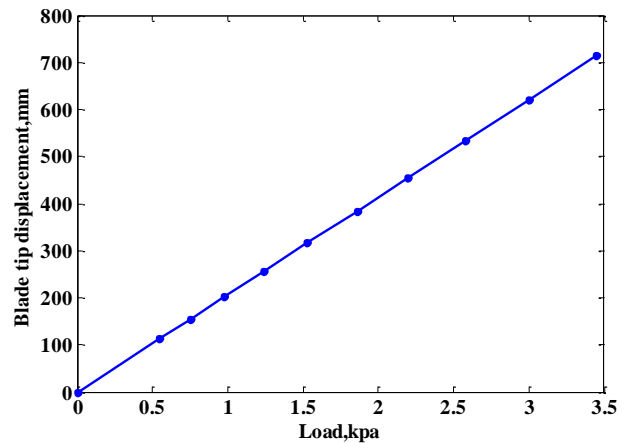


Figure 8: Relationship between load and tip displacement

## 5 CONCLUSIONS

A mixed airfoil composite blade for a 10KW horizontal fixed-pitch variable-speed turbine was designed based on BEM, it is concluded that the BEM theory is efficient in predicting rotor aerodynamic characteristics. The structural analysis was performed to evaluate the proposed design configuration by using the FE modelling method at the extreme wind conditions. The methodologies presented here can be utilized and adopted for further aeroelastic analysis.

## REFERENCES

- [1] H.Erich, Wind Turbines: Fundamentals, Technologies, Application, Economics, 2nd edition edn. Springer,2006.
- [2] B.Tony, S. David,J.Nick, B.Ervin, Wind Energy Handbook.John Wiley & Sons Ltd,2001.
- [3] J.Manwell,J.McGowan, J, Wind energy explained: theory, design and application second eddition,John Wiley & Sons Inc,2009.
- [4] D'Angelo S, Timmer W.A.,"Two wind turbines dedicated airfoils tested in two different wind tunnels:comparison and results", Windpoer'95 Conference, Washington D.C.USA,1995, March 26-30.
- [5] J.Tangler, K.J. David, "Wind Turbine Post-Stall Airfoil Performance Characteristics Guidelines for Blade-Element Momentum Methods", NREL/CP-500-36900,2004.
- [6] Ladean R. McKittrick, Douglas S. Cairns and John Mandell, etc. "Analysis of a composite blade design for the AOC1550 wind turbine using a finite element model[R]". California: Sandia National Laboratories, 2001.
- [7] Dassault Systèmes Simulia Corp. ABAQUS User's Manual, Providence, RI, 2010.
- [8] IEC 61400-1:2005(E). Wind turbines–Part 1:Design requirements[S]. Switzerland: International Electrotechnical Commission, 2005.